Published in final edited form as:
*Circulation*. 2006 January 24; 113(3): 394–404. doi:10.1161/CIRCULATIONAHA.105.521450.

# Contrast-Enhanced Multidetector Computed Tomography Viability Imaging After Myocardial Infarction:

## Characterization of Myocyte Death, Microvascular Obstruction, and Chronic Scar

**Albert C. Lardo, PhD**, **Marco A.S. Cordeiro, MD, PhD**, **Caterina Silva, MD**, **Luciano C. Amado, MD**, **Richard T. George, MD**, **Anastasios P. Saliaris, MD**, **Karl H. Schuleri, MD**, **Veronica R. Fernandes, MD**, **Menekhem Zviman, PhD**, **Saman Nazarian, MD**, **Henry R. Halperin, MD, MA**, **Katherine C. Wu, MD**, **Joshua M. Hare, MD**, and **Joao A.C. Lima, MD**
Department of Medicine, Division of Cardiology (A.C.L., M.A.S.C., C.S., L.C.A., R.T.G., A.P.S., K.H.S., V.R.F., M.Z., S.N., H.R.H., K.C.W., J.M.H., J.A.C.L.), Department of Biomedical Engineering (A.C.L., H.R.H., J.M.H.), Department of Surgery (A.C.L.), Department of Radiology (A.C.L., H.R.H., J.A.C.L.), and Institute of Cellular Engineering (J.M.H., L.C.A., A.P.S., K.H.S.), Johns Hopkins University School of Medicine, Baltimore, Md.

## Abstract

**Background—**The ability to distinguish dysfunctional but viable myocardium from nonviable tissue has important prognostic implications after myocardial infarction. The purpose of this study was to validate the accuracy of contrast-enhanced multidetector computed tomography (MDCT) for quantifying myocardial necrosis, microvascular obstruction, and chronic scar after occlusion/reperfusion myocardial infarction.

**Methods and Results—**Ten dogs and 7 pigs underwent balloon occlusion of the left anterior descending coronary artery (LAD) followed by reperfusion. Contrast-enhanced (Visipaque, 150 mL, 325 mg/mL) MDCT (0.5 mm × 32 slice) was performed before occlusion and 90 minutes (canine) or 8 weeks (porcine) after reperfusion. MDCT images were analyzed to define infarct size/extent and microvascular obstruction and compared with postmortem myocardial staining (triphenyltetrazolium chloride) and microsphere blood flow measurements. Acute and chronic infarcts by MDCT were characterized by hyperenhancement, whereas regions of microvascular obstruction were characterized by hypoenhancement. MDCT infarct volume compared well with triphenyltetrazolium chloride staining (acute infarcts 21.1±7.2% versus 20.4±7.4%, mean difference 0.7%; chronic infarcts 4.15±1.93% versus 4.92±2.06%, mean difference −0.76%) and accurately reflected morphology and the transmural extent of injury in all animals. Peak hyperenhancement of infarcted regions occurred ≈5 minutes after contrast injection. MDCT-derived regions of microvascular obstruction were also identified accurately in acute studies and correlated with reduced flow regions as measured by microsphere blood flow.

**Conclusions—**The spatial extent of acute and healed myocardial infarction can be determined and quantified accurately with contrast-enhanced MDCT. This feature, combined with existing



Correspondence to Albert C. Lardo, PhD, FAHA, Johns Hopkins School of Medicine, Division of Cardiology, 720 Rutland Ave, 1042 Ross Bldg, Baltimore, MD 21205. al@jhmi.edu.



Presented in part at the 2004 American Heart Association Scientific Sessions, New Orleans, La, November 7–10, 2004, and published in abstract form (*Circulation*. 2004;110(suppl III):III-522).

**The online-only Data Supplement can be found at http://circ.ahajournals.org/cgi/content/full/113/3/394/DC1**.

**Disclosures**
Drs Lardo and Lima receive research support from Toshiba, Inc. The other authors report no conflicts.

high-resolution MDCT coronary angiography, may have important implications for the comprehensive assessment of cardiovascular disease.

### Keywords

tomography; heart diseases; imaging; contrast media; myocardial infarction

The ability to distinguish dysfunctional but viable myocardium from nonviable tissue after acute or chronic ischemia has important implications for the therapeutic management of patients with coronary artery disease. In the acute phase, myocardial revascularization in patients with viable myocardium can improve ventricular dysfunction[1] and long-term survival,[2] whereas revascularization in patients with predominantly nonviable myocardium increases exposure to the unnecessary risk of invasive procedures and increases late mortality.[3] In setting of chronic ischemia, image-based characterization of myocardial scar morphology can identify those patients with hibernating myocardium who may achieve functional systolic recovery with revascularization.[4] Furthermore, the ability to image healed myocardial infarction may possibly identify patients susceptible to life-threatening arrhythmias and sudden cardiac death. The assessment of both acute and chronic myocardial viability and infarct morphology with delayed contrast-enhanced MRI has been well validated over the past several years[4,5] and is performed routinely by several clinical cardiac MRI centers. As the clinical indications for implantable cardiac defibrillators and biventricular pacing therapy continue to expand, however, development and validation of alternative imaging modalities with similar anatomic, functional, and viability imaging capabilities are needed to accommodate this growing population of patients who are not candidates for MRI. Moreover, the limited spatial resolution of MRI methods in the z or axial direction (slice thickness) remains an important factor for the accurate assessment of nonviable myocardial tissue by MRI.[5]

The recent advent of multidetector computed tomography (MDCT) technology has greatly improved spatial and temporal resolution over conventional single-slice computed tomography imaging and has expanded its potential for a more comprehensive evaluation of cardiovascular diseases. To date, however, the clinical application of cardiac MDCT has been largely relegated to the assessment of coronary atherosclerosis.[6–8] A limited number of previous studies have reported detection of iodinated contrast material within myocardium after myocardial damage[9]; however, a complete quantitative assessment of myocardial necrosis, microvascular obstruction, and collagenous chronic myocardial scar with modern MDCT technology has not been reported previously. Accordingly, the purpose of the present study was to determine the utility of 0.5-mm×32 slices MDCT to assess myocardial viability and characterize morphological infarct parameters such as size, transmurality, and microvascular obstruction in occlusion/reperfusion animal models of acute and chronic myocardial infarction.

## Methods

### Animal Preparation and Experimental Protocol

All procedures were approved by the Animal Use and Care Committee at the Johns Hopkins University School of Medicine.

**Acute Canine Model—**Ten mongrel dogs (mean weight 32±2.3 kg) were anesthetized with thiopental (26 mg/kg IV), intubated, and mechanically ventilated with isoflurane anesthesia during catheterization and MDCT scanning. Through a right femoral artery catheter sheath, a 7F pigtail catheter was placed into the left ventricle (LV) and used for both microsphere administration and withdrawal of reference blood samples, as well as for blood

pressure monitoring. The left anterior descending coronary artery (LAD) was accessed with a JR 4 catheter introduced through a right carotid arterial sheath, and baseline coronary angiography was performed to demonstrate LAD patency. A 3-mm angioplasty balloon was then positioned immediately proximal to the first diagonal LAD vessel and inflated to 4 to 6 atm to achieve vessel occlusion for a period of 90 minutes, followed by reperfusion.

Regional microsphere blood flow (MBF) was measured by injection of 15-μm–diameter neutron-activated microspheres (BioPal, Worchester, Mass)[10] containing samarium, lanthanum, antimony, europium, lutetium, rhenium, iridium, or gold spheres (≈7.5 million spheres per injection) at multiple time points throughout the protocol: baseline (before LAD occlusion), early occlusion (5 minutes after occlusion), late occlusion (5 minutes before reperfusion), early reperfusion (5 minutes after reperfusion), and late perfusion (5 minutes before animals were euthanized). At each injection interval, microsphere blood samples were collected with a syringe infusion pump at a rate of 2.1 mL/min. The pericardium and sternotomy were then closed, and the animal was transported to the MDCT scanner room with a portable respirator. At the conclusion of the imaging protocol, thioflavin S was injected arterially for postmortem delineation of microvascular obstruction and allowed to circulate for ≈90 seconds (n=3). Animals were then euthanized by 200 mg/kg pentobarbital overdose, and the heart was immediately removed and sectioned into short-axis slices 10 mm thick from the apex toward the base of the heart. Myocardial sections were then submerged and incubated in a 1% solution of triphenyltetrazolium chloride (TTC) for 20 minutes at 37°C and photographed under room light. Regions that failed to stain with TTC were designated TTC-negative or infarcted regions. After postmortem photography, myocardial slices were sectioned into radial segments for MBF analysis. Myocardial and reference blood samples were weighed and processed by established microsphere counting and flow calculation methods.[10] Figure 1a summarizes the experimental protocol for the acute canine experiments.

**Chronic Porcine Model—**Seven pigs were initially sedated with ketamine hydrochloride 200 to 400 mg IV and then anesthetized with thiopental (26 mg/kg IV), intubated, and mechanically ventilated with isoflurane anesthesia. Through a right femoral artery catheter sheath, a 7F pigtail catheter was placed into the LV for blood pressure monitoring. The LAD coronary artery was accessed with a JR 4 catheter introduced through a right carotid arterial sheath, and baseline coronary angiography was performed to demonstrate LAD artery patency. A 3-mm angioplasty balloon was then positioned immediately proximal to the second diagonal LAD vessel and inflated to 4 to 6 atm to achieve vessel occlusion for a period of 60 minutes, followed by reperfusion. Animals were monitored until full recovery and then were returned to housing. Eight weeks after infarction, animals were again anesthetized with thiopental (26 mg/kg IV), intubated, and mechanically ventilated with isoflurane anesthesia for MDCT imaging. As with the acute canine studies, the heart was removed after MDCT imaging for sectioning and TTC staining (Figure 1b).

## MDCT Imaging Protocol

MDCT imaging was performed with a 0.5-mm×32-detector scanner (Aquilion32, Toshiba Medical Systems Corporation). Baseline MDCT imaging was performed before infarct both during and 5 minutes after contrast injection in 3 animals to serve as baseline control points. Animals received intravenous propranolol (2 to 5 mg IV) 30 minutes after reperfusion to achieve a heart rate <100 bpm and intravenous lidocaine (1 mg/kg) for postinfarct arrhythmias as needed to ensure consistent cardiac gating. Mean heart rate during the MDCT examination was 96±10 and 92±8 bpm for acute and chronic animals, respectively. After scout acquisition and slice prescription, a 150-mL bolus of iodixanol (Visipaque 320, Amersham Health) was injected intravenously at a rate of 5 mL/s, followed by a 30-mL

saline chaser. As the signal in the ascending aorta reached a predefined threshold of 150 Hounsfield units (detected by a bolus tracking sensor in the ascending aorta), respiration was suspended and imaging performed with a retrospectively gated cardiac MDCT protocol (gantry rotation time=400 ms, detector collimation=0.5 mm×32, pitch=7.2, tube voltage=135 kV, tube current=420 mA, and scanning field of view=13.2 mm). After the initial first-pass contrast scan, the postinfarct imaging protocol was repeated every 5 minutes over 40 minutes to characterize the temporal course of contrast agent kinetics in the infarct and remote myocardium.

**Image Reconstruction—**Simultaneously recorded surface ECGs were used to assign source images to the respective phases of the cardiac cycle. Multiple phases of 4 different myocardial slices representing the infarct were inspected to determine the optimal phase (minimal cardiac motion) for reconstruction and infarct assessment. Accordingly, axial images were reconstructed at a 0.5-mm slice thickness and cardiac phase of 75% by a multisegment reconstruction algorithm. Additionally, phase data at multiple axial slices were reconstructed from 0% to 90% of the cardiac cycle in 2% increments for assessment of global function parameters.

### MDCT Image and Data Analysis

MDCT images were analyzed with a custom cardiac function software package (Toshiba Medical, Inc). For each slice, endocardial and epicardial borders were defined with an automated border-detection algorithm, and global function parameters (myocardial mass and ejection fraction) were calculated. The spatial extents of myocardial damage and microvascular obstruction for both MDCT and postmortem photography were determined by hand planimetry for each myocardial slice and expressed as a volume ratio of the LV. For an individual axial slice, the infarct region was defined as the sum of the hyperenhanced and hypoenhanced regions, with hyperenhancement and hypoenhancement defined and hand-traced by an experienced operator. Contrast agent kinetics was assessed by tracking signal intensity of the infarct region, LV chamber, and remote myocardial region (adjacent LV free wall and midventricular septum) over 40 minutes. Direct slice-by-slice comparisons of MDCT and TTC images were accomplished with multiplanar reconstructions of axial slices that matched the short-axis postmortem myocardial slices (Vital Images, Inc). For acute studies, tissue samples for MBF measurements were extracted from remote and injured myocardial segments and matched with blood samples collected at multiple time points throughout the study and compared with similar MDCT myocardial regions.

### Statistical Analysis

Agreement between MDCT- and TTC-derived infarct size, for both acute and chronic data sets, was assessed by Bland-Altman analysis and expressed as mean±SD difference between the 2 methods at 95% CI.[11] The Wilcoxon signed rank test was performed to determine whether there were significant differences in MBF and signal density between remote and infarct regions in both acute and chronic studies. The Wilcoxon signed rank test is a robust nonparametric test used to test the median difference in paired data.[12] Statistical significance was defined as a 2-sided probability value $<0.05$.

## Results

### Hemodynamics and Global Function

Two animals with acute infarcts developed ventricular fibrillation and died during the balloon occlusion phase of the infarct model. Another acute animal died during MDCT scanning after the infarct. The respective preinfarct and postinfarct hemodynamic parameters for acute studies were as follows: systolic blood pressure 100±9 and 93±12 mm

Hg, diastolic blood pressure 67±17 and 56±15 mm Hg, heart rate 113±14 and 115±15 bpm, $O_2$ saturation 99±1% and 97±2%, and ejection fraction 49±3% and 25±8%.

## MDCT Infarct Imaging

**Acute Canine Model—**Preinfarct contrast-enhanced MDCT myocardial imaging during first pass (Figure 2a) and 5 minutes after contrast injection (Figure 2b) demonstrated homogenous and uniform myocardial opacification with no indication of focal myocardial hyperenhancement or hypoenhancement in the LAD bed. Postinfarct MDCT imaging identified myocardial lesions characterized by well-delineated hyperintense myocardial segments 5 minutes after contrast injection in all animals studied (Figures 2c and 3). Mean signal intensity for infarcted and remote myocardium 5 minutes after contrast was 260.5±56.5 and 133.8±10.8 Hounsfield units (HU), respectively ($P$=0.018). The geometric and spatial extent of myocardial damage could also be easily appreciated qualitatively in all animals with segmented maximal intensity projection 3D reconstruction of 0.5-mm-slice data (see online Movie Supplement). Visual (Figure 4a through 4h) and quantitative (Figure 4i) analyses of infarct signal intensity over time demonstrated peak intensity 5 minutes after contrast injection, with subsequent washout over at least 40 minutes in proportion to blood pool and remote myocardial clearance. Although infarct signal density decreased over this time interval, MDCT-defined infarct size remained unchanged. Direct comparisons of reconstructed slice-matched MDCT-and TTC-stained images showed excellent correlation with infarct morphology (Figures 5a, 5b, and 5d) and accurately predicted the actual transmural extent of myocardial injury as determined by TTC in 35 of 35 postmortem slices (9 transmural and 27 nontransmural). Additionally, Bland-Altman analysis showed MDCT infarct volume ratios matched well with those measured by postmortem TTC (21.4±% versus 20.8%, mean difference 0.7%, 95% CI −2.04 to 3.44; Figure 5e).

MDCT-defined regions of microvascular obstruction were identified in 3 of 7 animals and were also time dependent. The mean signal density of microvascular obstruction and remote myocardial regions 5 minutes after contrast were 73.3±18 and 133.8±10.8 HU, respectively ($P$=0.0156). Figure 5a represents an example of simultaneous MDCT microvascular obstruction and infarct imaging that compared well with thioflavin S and TTC staining (Figure 5c, arrows). Microvascular obstruction regions were most prominent early after contrast injection (Figure 6a) and consistently showed progressive increases in signal intensity over time (Figure 6b through 6e and Figure 6f). MDCT-defined regions of microvascular obstruction at 5 minutes after contrast injection compared well with thioflavin S–derived measurements (7.2±1.2% versus 8.5±2.1%, mean difference 1.2%). MBF measurements taken at late reperfusion (just before MDCT) confirmed decreased myocardial blood flow in regions of microvascular obstruction compared with remote myocardial segments, respectively (0.05±0.02 versus 1.8±0.3 mL $\cdot$ $g^{-1}$ $\cdot$ $min^{-1}$, $P$=0.016).

**Chronic Porcine Model—**Similar to acute infarcts, myocardial scar by MDCT was characterized by subendocardial regions of hyperenhancement in the LAD myocardial territory (Figure 7a) that also reached maximal intensity ≈5 minutes after contrast injection. Mean signal intensity for infarcted and remote myocardium 5 minutes after contrast was 181±39 and 97±15 HU, respectively ($P$=0.028). Chronic infarct volume by MDCT also compared well with TTC staining (Figures 7b and 7c), with a qualitative trend toward underestimation by MDCT (4.15±1.93% versus 4.91±2.06%, mean difference −0.763%, 95% CI −1.54 to 0.02; Figures 7d and 7e).

## Histopathology Findings

Myocardial samples extracted from the infarct (TTC-negative), remote, and border regions (interface that contains both TTC-negative and TTC-positive regions) in acute animals were

submitted for histopathology analysis. Hematoxylin and eosin stains of the remote or TTC-positive areas demonstrated no structural alterations compared with normal canine myocardium, including unremarkable myocytes and blood vessels (Figure 8c). In the TTC-negative (infarct) region, multiple abnormalities were appreciated that were consistent with acute myocyte necrosis, including extensive contraction band necrosis without evidence of nuclear changes (Figure 8d, arrow), as well as waves of neutrophils migrating outside capillaries and accumulated within interstitial spaces (arrow). In the border-zone region, normal myocytes were separated by large waves of neutrophilic infiltrate and contraction band necrosis (Figure 8e).

## Discussion

### Main Findings

The major finding of the present study is that delayed MDCT myocardial imaging (0.5 mm×32 slices) can accurately identify and characterize morphological features of acute and healed myocardial infarction, including infarct size, transmurality, and the presence of microvascular obstruction and collagenous scar. Infarcted myocardial tissue by MDCT is characterized by well-delineated hyperenhanced regions that reach peak intensity ≈5 minutes after contrast injection, whereas regions of microvascular obstruction by MDCT are characterized by hypoenhancement on early imaging and are also time dependent. These findings may have important implications for the comprehensive assessment of patients with coronary artery disease and myocardial infarction.

It is well known that patient prognosis after acute myocardial infarction is directly related to the extent of myocardial injury produced during coronary occlusion.[13] Indirect assessment of the degree of myocardial damage postinfarction is accomplished by echocardiography, 12-lead ECG analysis, and contrast ventriculography, whereas imaging techniques such as $^{99m}$Tc sestamibi and contrast-enhanced MRI can measure infarct size directly.[14–16] Mechanisms of myocardial damage after acute myocardial infarction are complex and involve several dynamic simultaneous physiological processes. In addition to the importance of infarct extent/size for predicting functional recovery after acute myocardial infarction, it has been shown that the presence of microvascular obstruction or “no reflow” zones at the core of the injured myocardial territory is an independent predictor of poor clinical outcome.[17,18] In this regard, the possibility of directly measuring infarct size and microvascular obstruction in conjunction with coronary imaging represents an undisputed advantage of MDCT over other imaging technologies.

Myocardial viability imaging in the chronic setting has clinical relevance to patients with reversible myocardial dysfunction and chronic ischemia. In this group, it has been shown that the transmural extent of hyperenhancement by MRI directly predicts the likelihood of functional improvement with revascularization.[4]

### Computed Tomography Myocardial Viability Imaging

The potential role of computed tomography for the detection of acute myocardial infarction in explanted hearts and experimental animal models was first noted in the late 1970s and explored by Higgins et al.[19–24] In this series of work, it was first shown in explanted hearts that acute infarcts were detectable by computed tomography as regions of reduced signal density (hypoenhancement) compared with normal myocardium.[19] Higgins et al[9,25] performed fluorescent excitation analysis to demonstrate preferential uptake of contrast media in myocardial segments damaged by acute ischemia. More recently, Hoffmann et al[26] performed MDCT (4×1.25 mm) in a pig model of nonreperfused myocardial infarction and

showed a good correlation between TTC-derived infarct region and MDCT regions of low signal density or hypoenhancement.

MDCT infarct assessment based on regional hypoenhancement from first-pass imaging has important limitations. Regions of hypoenhancement indicate myocardial segments that are underperfused owing to an obstructed infarct-related artery, microvascular obstruction in the acute setting, or diminished capillary density associated with scar formation chronically. Although it is reasonable that the region hypoenhancement by MDCT reflects the region of infarcted tissue in a model of coronary occlusion without reperfusion,[26] this relationship does not apply for reperfused infarcts, which have become much more common after the introduction of reperfusion therapy. In the present study, we sought to exploit previous reports of selective uptake of iodinated contrast agents in infarcted myocardium by performing delayed MDCT hyperenhancement infarct imaging for full characterization of infarct morphology in occlusion/reperfusion models of myocardial infarction. These results indicate that the addition of hypoenhanced and hyperenhanced myocardial regions best reflects the extent of myocardial injury.

### Comparison With MRI

Because of its high contrast-to-noise ratio, lack of ionizing radiation and nephrotoxic contrast, and its well-documented success in myocardial imaging, MRI is a highly attractive modality for myocardial viability imaging. However, this method also has some practical drawbacks compared with MDCT, including higher cost, more complex infrastructure, longer scanning times, and restriction to study patients with implanted electronic devices, which is especially relevant in patients with previous myocardial infarction. With respect to detailed tissue characterization for myocardial viability imaging, a very important advantage of MDCT is that signal density values are unique and determined by the physical properties of individual constituents of the heart, including blood and viable and nonviable myocardium, that result from direct attenuation of the x-ray beam by iodine molecules. Conversely, MRI hyperenhancement results from gadolinium-induced alterations of water proton relaxivity and thus is only an indirect measure of the amount and biodistribution of the contrast agent. This may have especially important implications for the accurate assessment of acute infarct size by MRI, because subendocardial interstitial edema is believed by some to accompany acute myocardial injury and to be responsible in part for overestimation of infarct size by MRI in the acute setting.[27]

Another important advantage of acute infarct imaging by MDCT over MRI is a greatly reduced slice thickness. Partial volume effects, which are artifacts associated with all tomographic imaging modalities, become particularly prominent when the slice thickness exceeds the size of the structure of interest and result in the averaging of all information contained in the slice into a single-projection– like image. The 0.5-mm slice thickness of MDCT technology is 10 to 20 times thinner than that used in typical MRI viability imaging studies, thereby greatly reducing partial volume effects. An additional and independent advantage of the small slice thickness by MDCT is greatly improved spatial resolution in the z axis. An MDCT 0.5-mm slice achieves near isotropic resolution, which allows for true 3D data and the ability to reconstruct any arbitrary slice orientation from the original stack of axial slices. This is especially practical for viability imaging, in which infarct morphology can vary substantially when slices are oriented even slightly oblique from a true short-axis view. In contrast, during MRI, the slices of interest must be acquired at the time of the scan, which greatly increases operator interaction and examination time.

Finally, the accuracy of MRI-derived assessment of myocardial infarct size has been shown to be dependent on the timing of image acquisition after the injection of Gd-DTPA.[28] The inversion time is a parameter in the delayed hyperenhancement MRI acquisition that

determines the optimal contrast between normal and injured myocardium and is a function of time after contrast injection. Thus, this parameter must be optimized for each acquisition after contrast injection. In comparison, MDCT parameters for viability imaging vary much less, which represents a significant practical advantage in high-output clinical settings.

## Potential Mechanism of Infarct Hyperenhancement and Hypoenhancement by MDCT

The mechanism of myocardial hyperenhancement and hypoenhancement in acutely injured myocardial territories after iodinated contrast administration is similar to that proposed for delayed gadolinium-enhanced MRI.[29] Under conditions of normal myocyte function, sarcolemmal membranes serve to exclude iodine from the intracellular space. After myocyte necrosis, however, membrane dysfunction ensues, and iodine molecules are able to penetrate the cell. Because 75% of the total myocardial volume is intracellular, large increases in the volume of distribution are achieved, which results in marked hyperenhancement relative to the noninjured myocytes. The mechanism of hyperenhancement of healed myocardial infarction or collagenous scar is thought to be related to an accumulation of contrast media in the interstitial space between collagen fibers and thus an increased volume of distribution compared with that of tightly packed myocytes.

The low signal intensity of microvascular obstruction regions despite restoration of normal flow through the infarct-related artery is explained by the death and subsequent cellular debris blockage of intramyocardial capillaries at the core of the damaged region. These obstructed capillaries do not allow contrast material to flow into the damaged bed, which results in a region of low signal intensity compared with normal myocardium. Over time, contrast material is able to penetrate this “no reflow” region, and the necrotic myocytes that reside in that myocardial territory then become hyperintense as iodine is internalized by the cell.

## Clinical Implications

The results of the present study have significant clinical implications. Acute MDCT viability imaging of troponin-positive patients in the emergency department setting could allow for rapid assessment of key morphological parameters of myocardial infarction that provide an immediate rationale for either aggressive revascularization or standard medical therapy. Because computed tomography systems are standard in the modern emergency department for the diagnosis and assessment of urgent noncardiac events, this approach could be both convenient and financially justifiable. Additionally, on the basis of the data reported in the present study, we are developing novel imaging protocols to perform MDCT viability imaging in patients undergoing MDCT coronary angiography. This protocol requires an additional delayed helical scan after coronary imaging, which is possible without prohibitive radiation or contrast exposure for 2 important reasons highlighted in this work: (1) infarct hyperenhancement reaches a maximum very quickly (5 minutes) after contrast injection, and thus, the same contrast bolus used to acquire the MDCT coronary angiogram can be used to enhance nonviable myocardial segments; and (2) unlike MDCT coronary angiographic applications that require a 0.5-mm slice thickness, MDCT images of the myocardium can be acquired with thicker slices (1 to 4 mm), which allows for a substantial reduction in radiation dose. However, the use of thicker slices to reduce radiation dose comes at the expense of a loss of isotropic resolution. We are currently developing optimal delayed MDCT imaging protocols for use in humans that balance slice thickness and radiation dose parameters.

Finally, as the clinical indications for automatic internal cardiac defibrillators and cardiac resynchronization devices continue to expand, there is a large and growing population of patients with contraindications to MRI. The ability to perform both MDCT angiography and

viability imaging could be extremely valuable in this group of patients with advanced cardiovascular disease.

## Study Limitations

The present study includes assessment of super-acute or 8-week experimentally produced infarcts only. Clinically, infarct characterization in the subacute phase (1 to 3 days after injury) is also very important for the application of this technique in the setting of acute coronary syndromes. Also, we did not provide histopathologic evidence of intracellular iodine in infarcted tissue as defined by MDCT and TTC in the present study; however, previous experimental work does suggest that iodine accumulates preferentially in irreversibly damaged myocytes.[9] Furthermore, because the time step for MDCT imaging in the protocol was 5 minutes, time points between 0 and 5 minutes after contrast injection were not acquired. Although multiple time points between 0 and 5 minutes would be ideal, a 5-minute time step appears to provide adequate time resolution to capture the infarct wash-in and washout kinetics

Lastly, the contrast injection used in the study for 30-kg dogs in average is approximately equivalent to a double contrast dose for an average-sized patient. Such a dose (150 mL) was selected for this study to ensure contrast material was not a limiting factor and that maximal infarct uptake was achieved for accurate characterization of contrast kinetics and infarct physiology in relation to histopathology. We have also successfully performed MDCT viability studies in the same infarct model using a 50-mL contrast dose and reduced radiation protocols (see Figure 9).

## Conclusions

The spatial extent of myocardial damage and microvascular obstruction can be accurately assessed with contrast-enhanced 0.5-mm ×32 MDCT in occlusion/reperfusion models of acute and chronic myocardial infarction. Infarct hyper-enhancement occurs quickly after contrast injection and clearly identifies the infarct borders. This feature, combined with existing high-resolution MDCT coronary angiography and other functional tests, may have important implications for the comprehensive assessment patients with advanced cardiovascular disease.

### CLINICAL PERSPECTIVE

This work has important clinical implications because it mirrors the MRI paradigm, which continues to establish itself as the “gold standard” for the assessment of infarct size and myocardial viability in cardiology practice. The obvious advantages of the multidetector computed tomography (MDCT) method relate to the convenience of coupling it to MDCT coronary angiography and the possibility of studying patients with defibrillators and multilead cardiac resynchronization therapy devices. The success of myocardial protection during and after myocardial infarction has led to an ever-increasing number of patients with advanced heart disease and chronic heart failure who require such devices and who would be the primary population to benefit from the methods reported in this study. Questions of viability and the need for repeated revascularization are of crucial importance to this group of patients. The long-term adoption of MDCT delayed enhancement techniques will depend on (1) further demonstration of its value in patients with advanced heart disease, (2) the ability to couple myocardial viability assessment with MDCT coronary angiography at acceptable levels of radiation (levels similar or below those required for a double isotope nuclear test, ie, ≤10 mSv), and (3) the availability and convenience of competing methods based on MRI, ultrasound, or nuclear technology targeted to assess myocardial viability in

patients with advanced heart failure. Thus, the present report has crucial potential importance to a large segment of patients with heart disease.

## Supplementary Material

Refer to Web version on PubMed Central for supplementary material.

## Acknowledgments

The authors would like to thank Marc Helushka, MD, for his interpretation of histopathology findings, William McCarthy, PhD, for his statistical guidance and assistance with data analysis, and Anthony DiPaula for his assistance with the animal model. This work was supported by a grant from the Donald W. Reynolds Cardiovascular Research Foundation, Toshiba Medical Systems, and National Institutes of Health grants AG025017, HL65455, and U54HL081028.

## References

1. Alderman EL, Fisher LD, Litwin P, Kaiser GC, Myers WO, Maynard C, Levine F, Schloss M. Results of coronary artery surgery in patients with poor left ventricular function (CASS). Circulation. 1983; 68:785–795. [PubMed: 6352078]
2. Pagley PR, Beller GA, Watson DD, Gimple LW, Ragosta M. Improved outcome after coronary bypass surgery in patients with ischemic cardiomyopathy and residual myocardial viability. Circulation. 1997; 96:793–800. [PubMed: 9264484]
3. Bax JJ, Schinkel AF, Boersma E, Rizzello V, Elhendy A, Maat A, Roelandt JR, van der Wall EE, Poldermans D. Early versus delayed revascularization in patients with ischemic cardiomyopathy and sub-stantial viability: impact on outcome. Circulation. 2003; 108(suppl I):II-39–II-42. [PubMed: 12970206]
4. Kim RJ, Wu E, Rafael A, Chen EL, Parker MA, Simonetti O, Klocke FJ, Bonow RO, Judd RM. The use of contrast-enhanced magnetic resonance imaging to identify reversible myocardial dysfunction. N Engl J Med. 2000; 343:1445–1453. [PubMed: 11078769]
5. Wu KC, Lima JA. Noninvasive imaging of myocardial viability: current techniques and future developments. Circ Res. 2003; 93:1146–1158. [PubMed: 14670830]
6. Nieman K, Oudkerk M, Rensing BJ, van Ooijen P, Munne A, van Geuns RJ, de Feyter PJ. Coronary angiography with multi-slice computed tomography. Lancet. 2001; 357:599–603. [PubMed: 11558487]
7. Nieman K, Cademartiri F, Lemos PA, Raaijmakers R, Pattynama PM, de Feyter PJ. Reliable noninvasive coronary angiography with fast submillimeter multislice spiral computed tomography. Circulation. 2002; 106:2051–2054. [PubMed: 12379572]
8. Achenbach S. Detection of coronary stenoses by multidetector computed tomography: it's all about resolution. J Am Coll Cardiol. 2004; 43:840–841. [PubMed: 14998626]
9. Higgins CB, Sovak M, Schmidt W, Siemers PT. Uptake of contrast materials by experimental acute myocardial infarctions: a preliminary report. Invest Radiol. 1978; 13:337–339. [PubMed: 689828]
10. Reinhardt CP, Dalhberg S, Tries MA, Marcel R, Leppo JA. Stable labeled microspheres to measure perfusion: validation of a neutron activation assay technique. Am J Physiol Heart Circ Physiol. 2001; 280:H108–H116. [PubMed: 11123224]
11. Bland JM, Altman DG. Statistical methods for assessing agreement between two methods of clinical measurement. Lancet. 1986; 1:307–310. [PubMed: 2868172]
12. Conover, WJ. Practical Nonparametric Statistics. 2nd ed. New York, NY: Wiley; 1980.
13. Multicenter Postinfarction Research Group. Risk stratification and survival after myocardial infarction. N Engl J Med. 1983; 309:331–336. [PubMed: 6866068]
14. Goldman MR, Brady TJ, Pykett IL, Burt CT, Buonanno FS, Kistler JP, Newhouse JH, Hinshaw WS, Pohost GM. Quantification of experimental myocardial infarction using nuclear magnetic resonance imaging and paramagnetic ion contrast enhancement in excised canine hearts. Circulation. 1982; 66:1012–1016. [PubMed: 6181904]

15. Judd RM, Lugo-Olivieri CH, Arai M, Kondo T, Croisille P, Lima JA, Mohan V, Becker LC, Zerhouni EA. Physiological basis of myocardial contrast enhancement in fast magnetic resonance images of 2-day-old reperfused canine infarcts. Circulation. 1995; 92:1902–1910. [PubMed: 7671375]

16. Lima JA, Judd RM, Bazille A, Schulman SP, Atalar E, Zerhouni EA. Regional heterogeneity of human myocardial infarcts demonstrated by contrast-enhanced MRI: potential mechanisms. Circulation. 1995; 92:1117–1125. [PubMed: 7648655]

17. Wu KC, Kim RJ, Bluemke DA, Rochitte CE, Zerhouni EA, Becker LC, Lima JA. Quantification and time course of microvascular obstruction by contrast-enhanced echocardiography and magnetic resonance imaging following acute myocardial infarction and reperfusion. J Am Coll Cardiol. 1998; 32:1756–1764. [PubMed: 9822106]

18. Ito H, Tomooka T, Sakai N, Yu H, Higashino Y, Fujii K, Masuyama T, Kitabatake A, Minamino T. Lack of myocardial perfusion immediately after successful thrombolysis: a predictor of poor recovery of left ventricular function in anterior myocardial infarction. Circulation. 1992; 85:1699–1705. [PubMed: 1572028]

19. Gray WR Jr, Parkey RW, Buja LM, Stokely EM, McAllister RE, Bonte FJ, Willerson JT. Computed tomography: in vitro evaluation of myocardial infarction. Radiology. 1977; 122:511–513. [PubMed: 834904]

20. Gray WR, Buja LM, Hagler HK, Parkey RW, Willerson JT. Computed tomography for localization and sizing of experimental acute myocardial infarcts. Circulation. 1978; 58:497–504. [PubMed: 679441]

21. Higgins CB, Siemers PT, Schmidt W, Newell JD. Evaluation of myocardial ischemic damage of various ages by computerized transmission tomography: time-dependent effects of contrast material. Circulation. 1979; 60:284–291. [PubMed: 445746]

22. Higgins CB, Siemers PT, Newell JD, Schmidt W. Role of iodinated contrast material in the evaluation of myocardial infarction by computerized transmission tomography. Invest Radiol. 1980; 15:S176–S182. [PubMed: 7203920]

23. Doherty PW, Lipton MJ, Berninger WH, Skioldebrand CG, Carlsson E, Redington RW. Detection and quantitation of myocardial infarction in vivo using transmission computed tomography. Circulation. 1981; 63:597–606. [PubMed: 7460246]

24. Huber DJ, Lapray JF, Hessel SJ. In vivo evaluation of experimental myocardial infarcts by ungated computed tomography. AJR Am J Roentgenol. 1981; 136:469–473. [PubMed: 6781279]

25. Higgins CB, Sovak M, Schmidt W, Siemers PT. Differential accumulation of radiopaque contrast material in acute myocardial infarction. Am J Cardiol. 1979; 43:47–51. [PubMed: 758769]

26. Hoffmann U, Millea R, Enzweiler C, Ferencik M, Gulick S, Titus J, Achenbach S, Kwait D, Sosnovik D, Brady TJ. Acute myocardial infarction: contrast-enhanced multi-detector row CT in a porcine model. Radiology. 2004; 231:697–701. [PubMed: 15118118]

27. Saeed M, Bremerich J, Wendland MF, Wyttenbach R, Weinmann HJ, Higgins CB. Reperfused myocardial infarction as seen with use of necrosis-specific versus standard extracellular MR contrast media in rats. Radiology. 1999; 213:247–257. [PubMed: 10540668]

28. Oshinski JN, Yang Z, Jones JR, Mata JF, French BA. Imaging time after Gd-DTPA injection is critical in using delayed enhancement to determine infarct size accurately with magnetic resonance imaging. Circulation. 2001; 104:2838–2842. [PubMed: 11733404]

29. Thomson LE, Kim RJ, Judd RM. Magnetic resonance imaging for the assessment of myocardial viability. J Magn Reson Imaging. 2004; 19:771–788. [PubMed: 15170783]

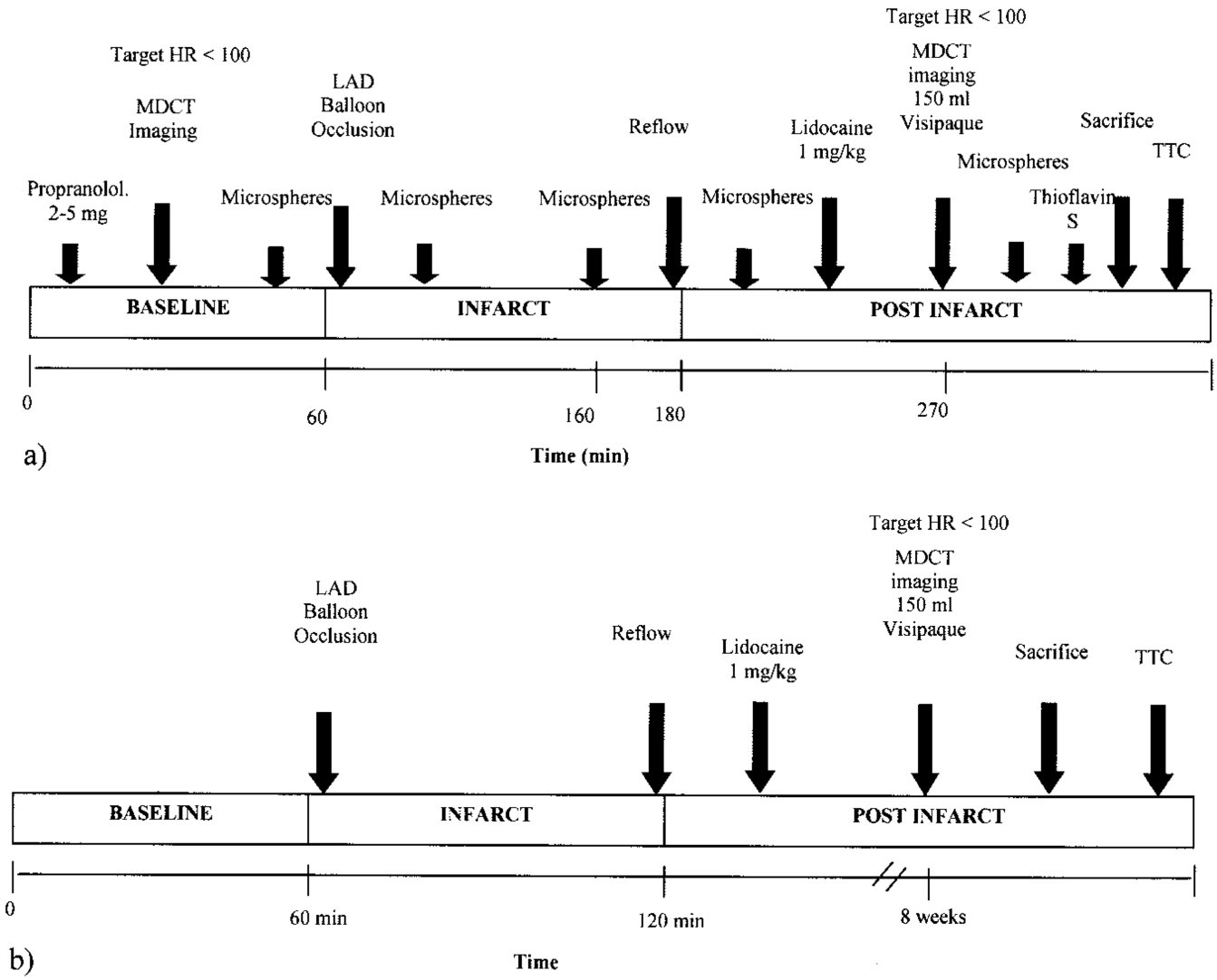


**Figure 1.**
Experimental protocol for (a) acute and (b) chronic experiments. HR indicates heart rate (in beats per minute).

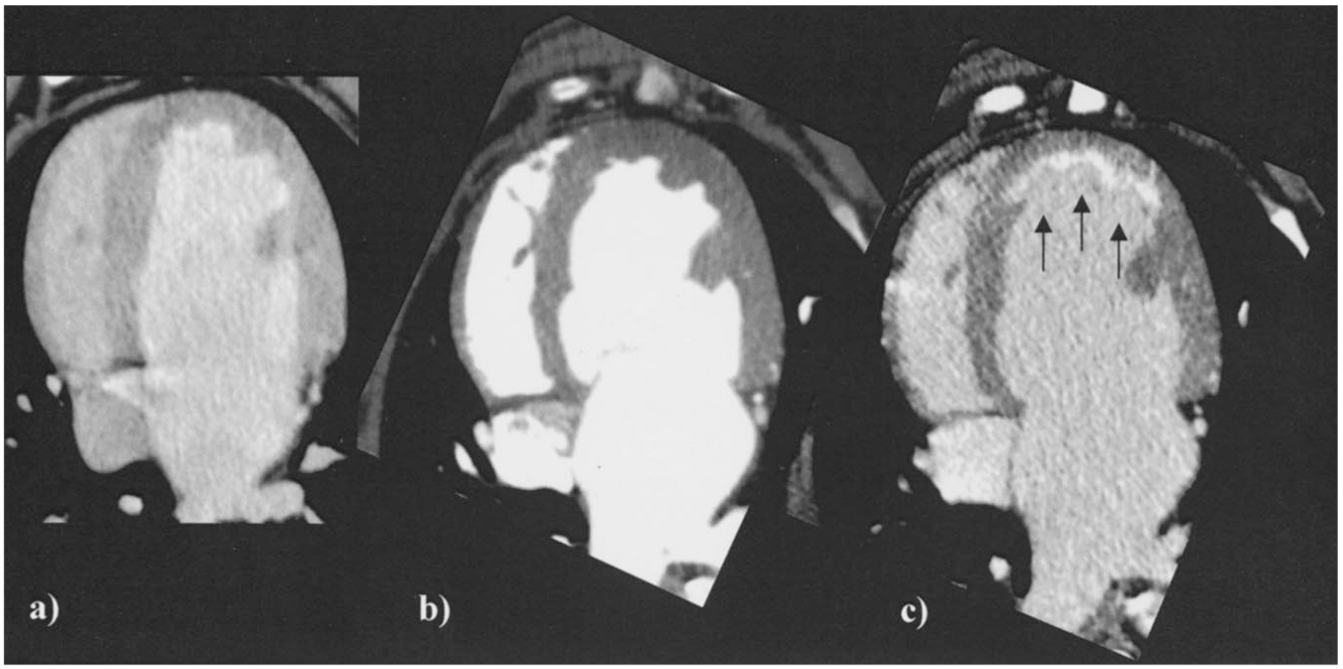


**Figure 2.**
Typical contrast-enhanced myocardial MDCT images showing axial slices (a) at baseline (preinfarct) 5 minutes after contrast, (b) postinfarct during first-pass contrast injection, and (c) postinfarct 5 minutes after contrast injection. The infarcted region is represented by the subendocardial anterior hyperintense region (arrows).

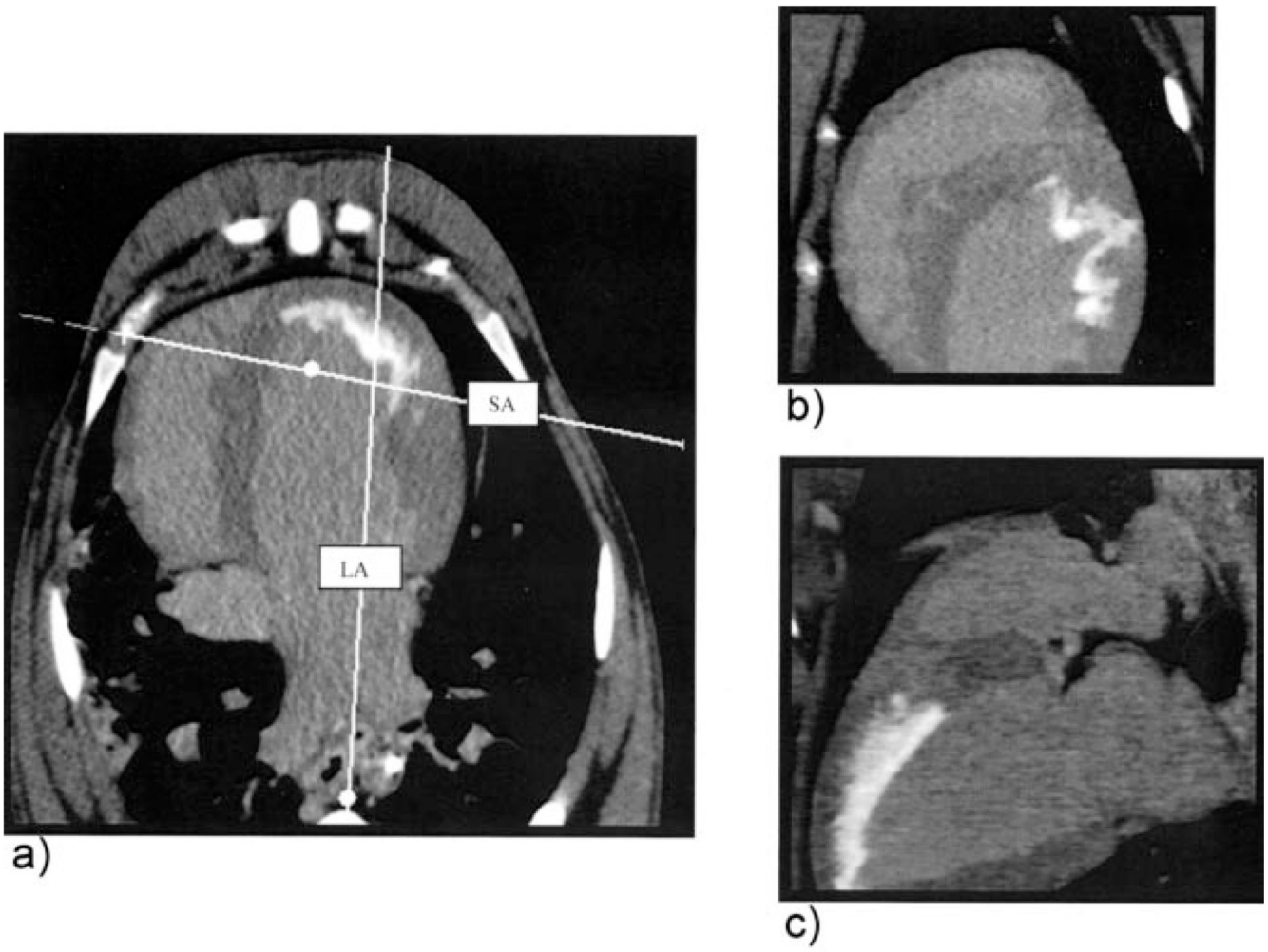


**Figure 3.**
a, Axial contrast-enhanced myocardial MDCT image showing orthogonal slice prescriptions representing (b) short-axis and (c) long-axis multiplanar reconstructions, respectively. The infarcted region is represented by the subendocardial anterolateral hyperintense region. LA indicates long axis; SA, short axis.

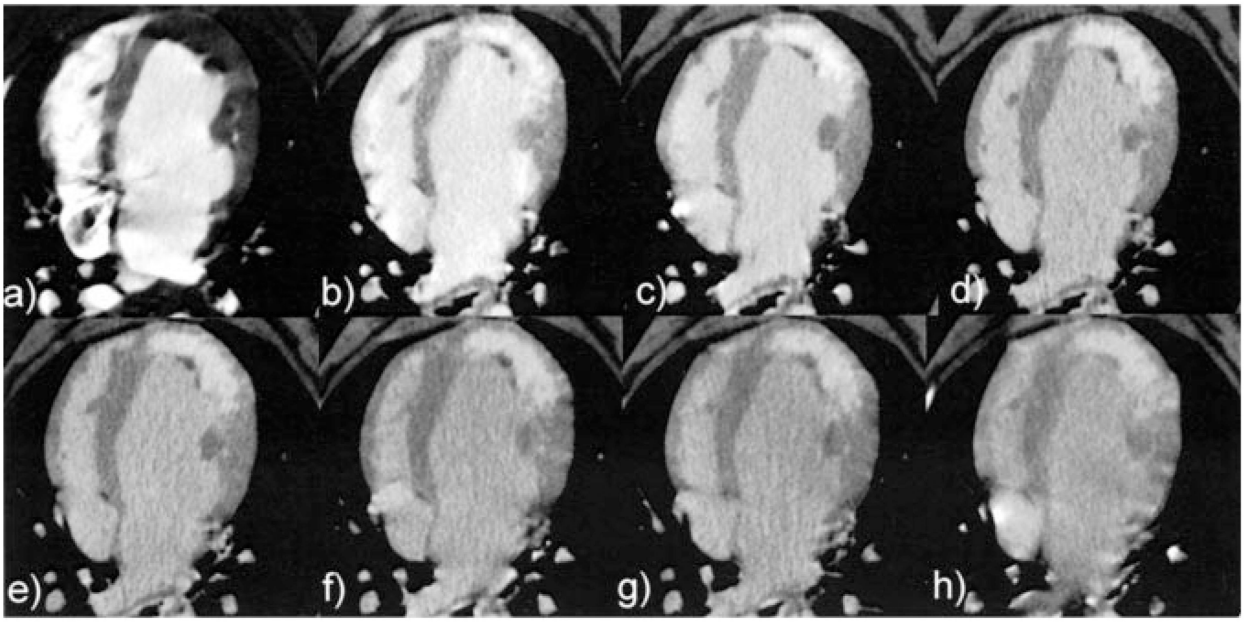


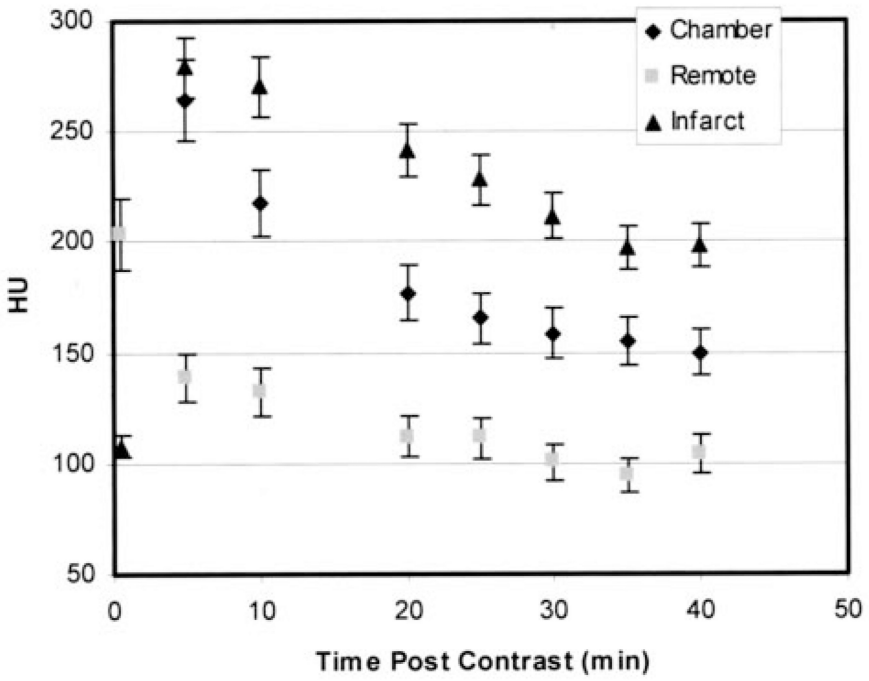


**Figure 4.**

a–h, Axial temporal image series demonstrating postreperfusion contrast agent kinetics after 150-mL injection of contrast. The first image (a) represents the first-pass image during contrast agent injection. Note that the signal density of the infarct in the first pass is substantially lower than that of the remote myocardium and indicates a subendocardial microvascular obstruction. Five minutes after injection (b), the signal density of the damaged myocardial region is significantly greater than that of the remote myocardium and washes out over time. The plot in (i) represents quantitative contrast kinetics for the LV chamber, remote myocardium, and infarct after contrast injection. As can be appreciated from (b), the infarct becomes well delineated and reaches peak enhancement at 5 minutes

after injection and then washes out in proportion to the chamber (blood pool) and remote myocardial signal.

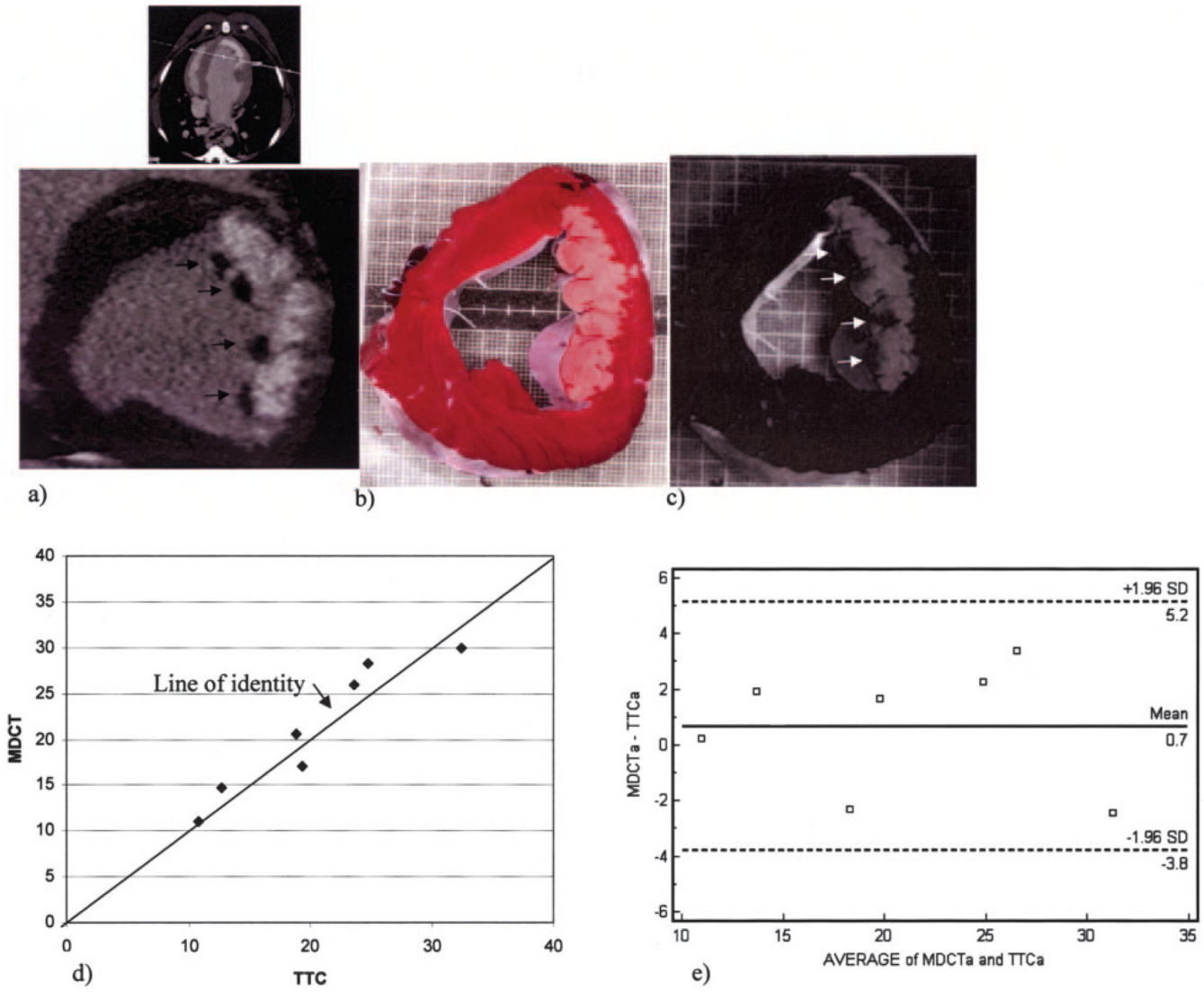


**Figure 5.**

MDCT and histopathologic staining comparison of infarct morphology. a, Reconstructed short-axis MDCT slice 5 minutes after contrast injection demonstrating a large anterolateral infarct (hyperenhanced region) with discrete endocardial regions of microvascular obstruction (4 arrows). b, TTC-stained slice; c, Thioflavin S and TTC staining of the same slice, which confirms the size and location of microvascular obstruction regions. d, Quantitative MDCT and TTC measurements of infarct size yielded good agreement, with points distributed around the line of identity. e, Mean difference of 0.7% by Bland-Altman analysis.

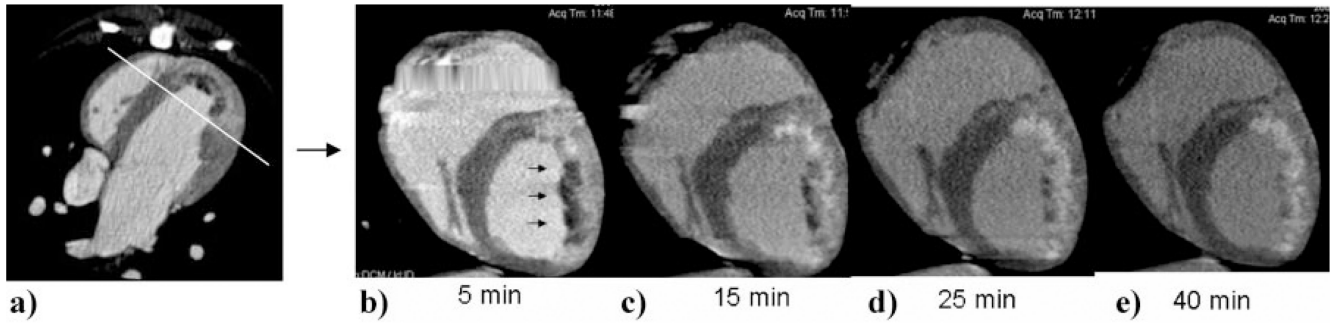


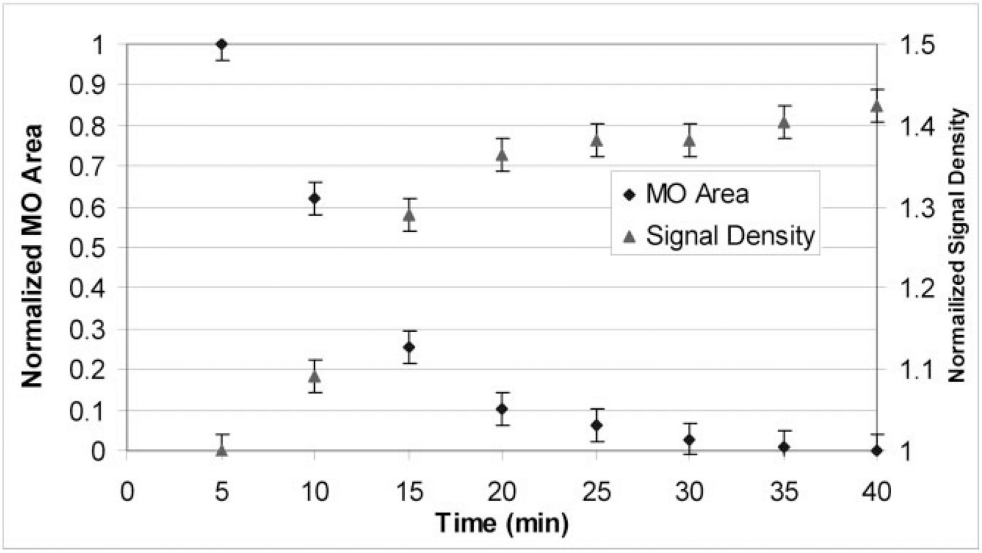


**Figure 6.**

a, Axial cardiac MDCT image 2 hours after LAD occlusion/reperfusion showing an orthogonal slice prescription. The large anterior region of low signal density represents a region of microvascular obstruction at the endocardial portion of the infarct. b through e, Short-axis reconstruction of the same slice over time to characterize changes in the region of microvascular obstruction (arrows). As can be appreciated, the region of low signal density is surrounded by a region of high signal density early after contrast injection and then slowly increases over time and eventually reaches the level of surrounding high signal density myocardium. f, Plot of both normalized size and signal density of the microvascular obstruction (MO) region over time.

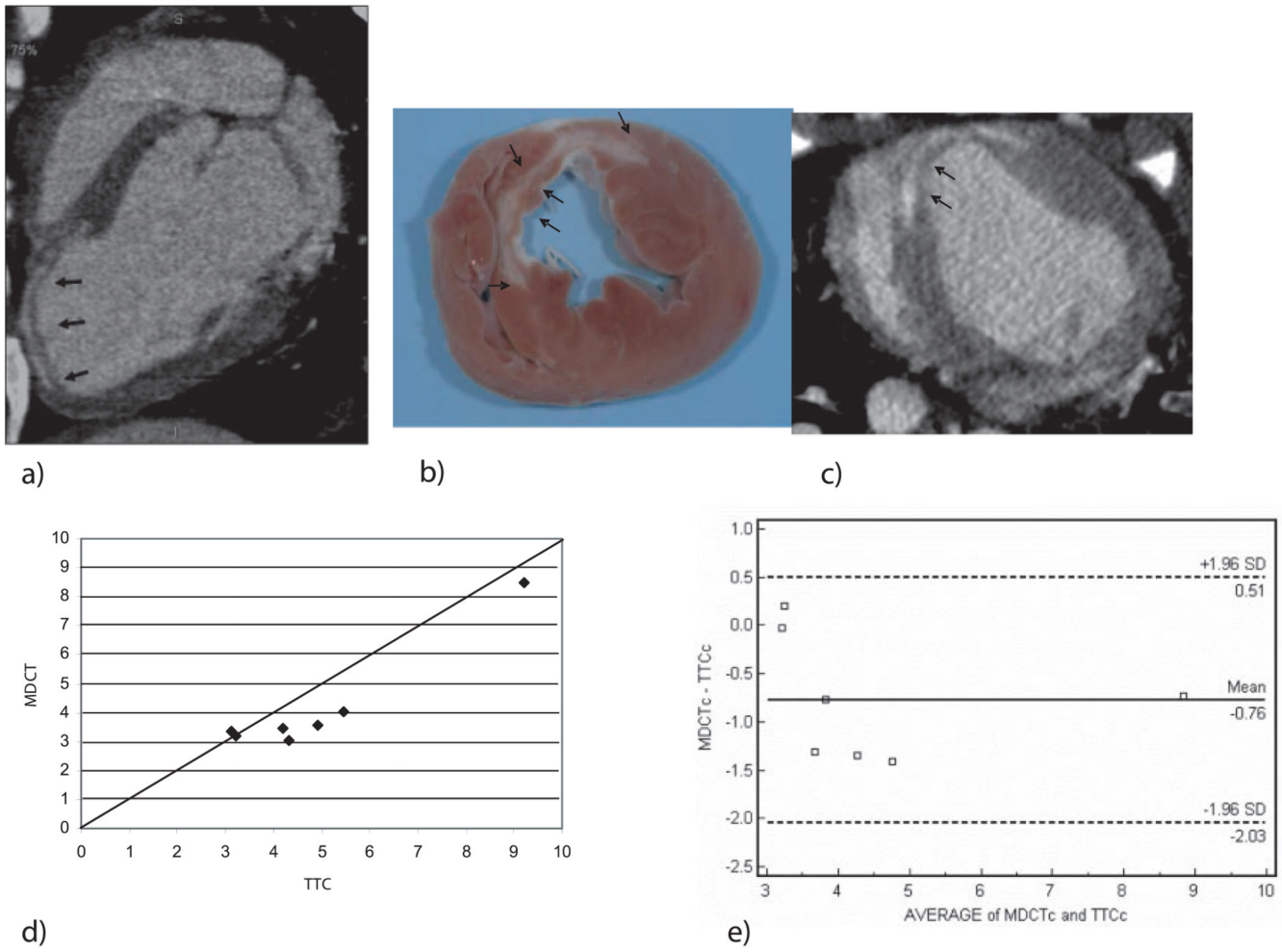


**Figure 7.**

a, Sagittal cardiac MDCT image of an 8-week-old infarct in a porcine model 5 minutes after contrast injection. b, Short-axis MDCT image and (c) corresponding gross examination photograph. d and e, Quantitative comparison of MDCT and gross examination/ TTC infarct size.

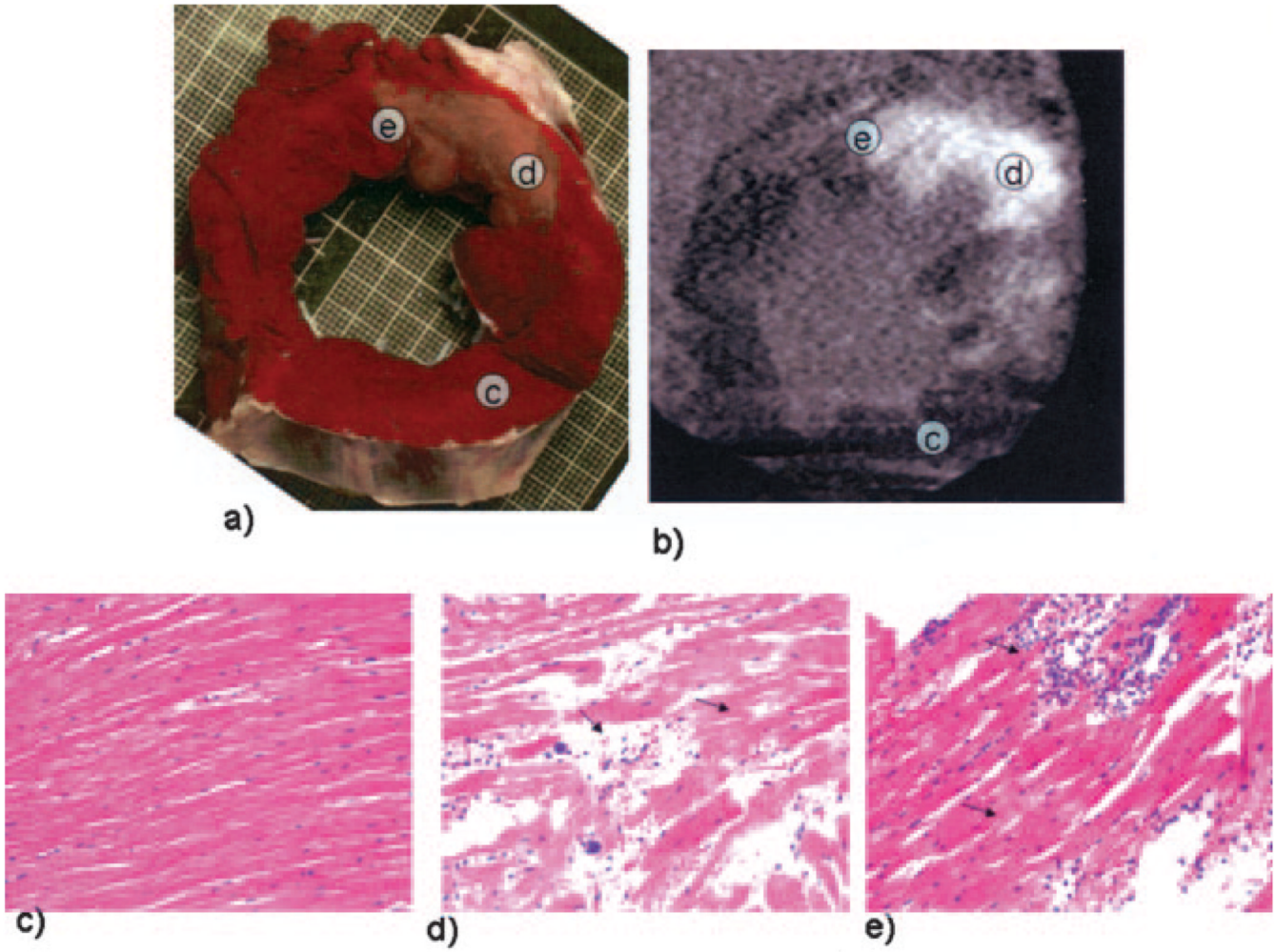


**Figure 8.**

TTC (a) and MDCT (b) images and hematoxylin and eosin histopathology analysis (c–e) from myocardial samples extracted ≈2 hours after the ischemic event. Samples were taken from remote, infarcted, and border regions. Remote myocardial areas (TTC-negative) demonstrate no change to the normal canine myocardial elements, including unremarkable myocytes and blood vessels (c). The TTC-negative (infarct) region demonstrated multiple changes that were consistent with acute myocyte necrosis, including extensive contraction band necrosis without evidence of nuclear changes (arrow) and waves of neutrophils leaving small blood vessels and collecting within interstitial spaces (arrow, d). In the border-zone region, normal myocytes were separated by large waves of neutrophilic infiltrate and contraction band necrosis (e).

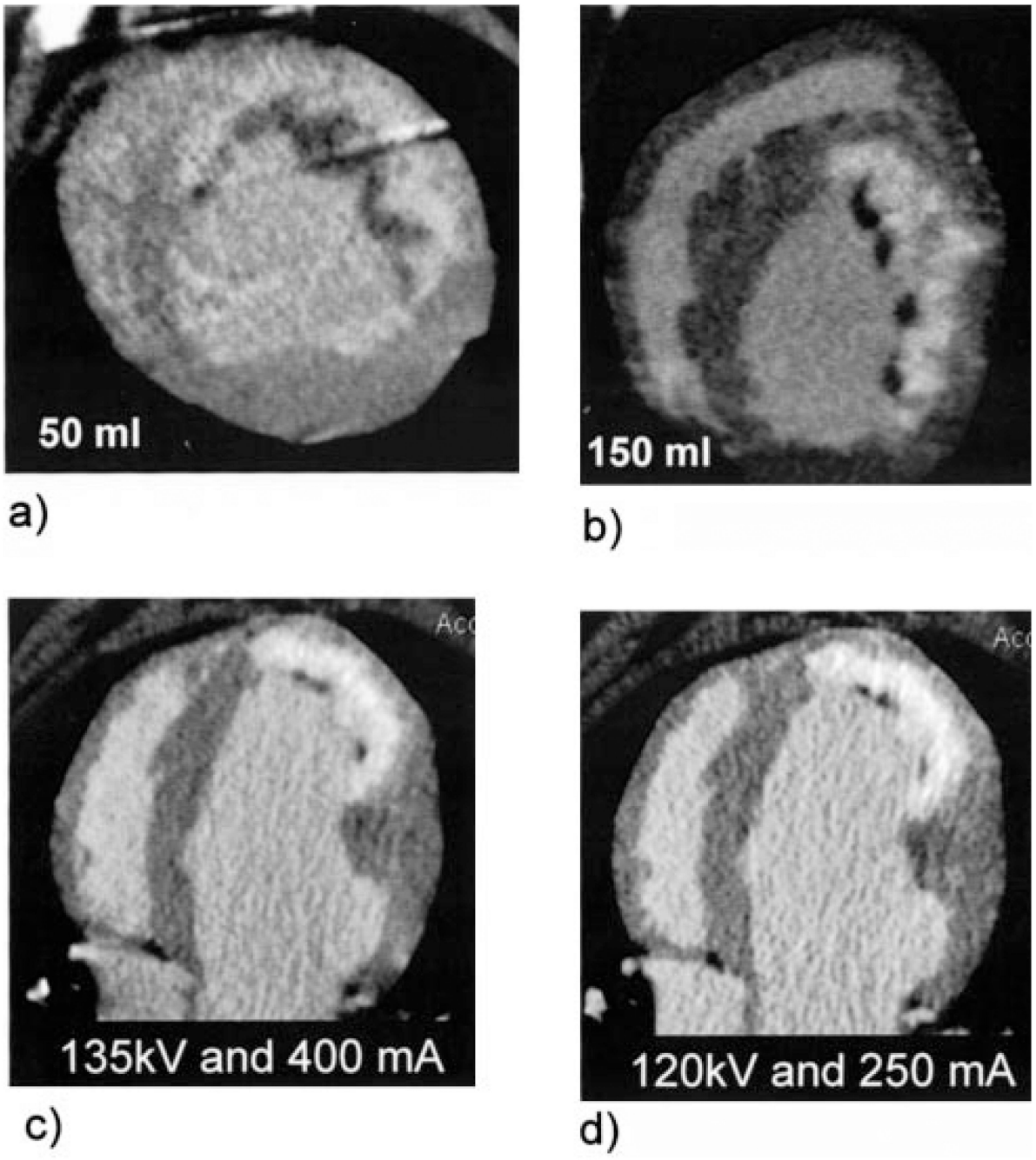


**Figure 9.**

Comparison of (a) low (50 mL) and (b) high dose (150 mL) MDCT infarct images 5 minutes after contrast injection. Panels c and d show identical slices acquired with 2 different imaging protocols to demonstrate the effect of radiation dose on image quality. The image in (c) was acquired with a relatively high radiation dose (135 kV and 400 mA, approximately equivalent to 3 REM), whereas the image in (b) was acquired with the clinical protocol used at our institution for CT coronary angiography (120 kV and 250 mA). Lower contrast and radiation does had no effect on the accuracy of quantitative infarct-size measurements.